

# Quantum phase crossover and chaos in generalized Jahn-Teller lattice model

Eva Majerníková<sup>1</sup> and Serge Shpyrko<sup>2</sup>‡

<sup>1</sup> Institute of Physics, Slovak Academy of Sciences, Dúbravská cesta 9, SK-84 511 Bratislava, Slovak Republic

<sup>2</sup>Institute for Nuclear Research, Ukrainian Academy of Sciences, pr. Nauki 47, Kiev, Ukraine

E-mail: eva.majernikova@savba.sk

**Abstract.** The generalized multispin Jahn-Teller model on a finite lattice or formally equivalent Dicke model extended to two long-wavelength coherent bosons of different frequencies is shown to exhibit a crossover between the polaron-modified "quasi-normal" and the squeezed "radiation" domains. We investigate effects of two kinds of interfering fluctuations on the phase crossover and on statistical characteristics of boson complex spectra: (i) Fluctuations in the *electron* subsystem- finite-size quantum fluctuations- are responsible for the dephasing of the coherence in the radiation domain and for the moderate occupation of the excited states in the normal domain. In the quasiclassical limit, radiation phase implies existence of a coherent acoustic super-radiant phase. (ii) Level-spacing fluctuations in excited *boson* level subsystem with strong level repulsions. Related probability distributions are shown to be non-universally spread between the limiting universal Wigner-Dyson and Poisson distributions. We proved that the difference in boson frequencies is responsible for reaching the most stochastic limit of the Wigner-Dyson distribution. Instanton lattice as a sequence of tunneling events in the most chaotic radiation domain exhibits maximal number of level-avoidings (repulsions). The non-universality of the distributions is caused by boson correlations which compete the level repulsions.

PACS numbers: 63.22.-m, 05.45.Mt, 73.43.Nq, 31.30.-i

Submitted to: *J. Phys. A: Math. Gen.*

‡ email: serge\_shp@yahoo.com

## 1. Introduction

The class of spin-boson lattice models with one [1, 2, 3, 4, 5, 6, 7, 8, 9] or two boson modes of different local symmetry [10, 11, 12, 13] gained a long-term interest in condensed matter physics and quantum optics. They exhibit a rich variety of interesting statistical properties as spectral chaos and quantum and thermodynamic phase transitions. The complex (chaos bearing) excited energy spectra are a consequence of multiple level repulsions and avoidings [14]. Recently, discovery of the exciton-polariton Bose-Einstein condensation in semiconductor microcavities [7, 15, 16, 17] contributed to this fascinating field.

An array of two-level atoms localized on a lattice and dipole-interacting with one long-wavelength boson (photon) mode – the Dicke model [5] – has been found to exhibit quantum and thermodynamic spontaneous phase transition in adiabatic approximation [5, 6, 7, 8, 9, 17, 18] from the effectively unexcited ”normal” phase to the ”super-radiant” phase, a macroscopically excited and highly collective state. A collective spontaneous emission of coherent radiation is due to the cooperative interaction of a large number of two-level localized atoms all excited to the upper state. Moreover, the Dicke model has been found to exhibit the Wigner-Dyson probability distribution of the nearest neighbour level spacings (NNLS) of excited boson spectra [9]. Generally, this type of fluctuations was intensively studied by the quantum chaology [14] for understanding the complex excited spectra of many-body systems [19].

There are several motivations for the present generalization to the multispin JT model and different frequencies of two boson modes:

- (a) Our preceding investigations [20, 21] of the ground state of the Jahn-Teller (JT) model resulted in finding features analogous to those of the Dicke model;
- (b) Investigation of characteristics of quantum chaos in  $E \otimes (b_1 + b_2)$  JT spectra [22] left open questions: we expect further enhancement of the level-spacing fluctuations due to the difference in the mode frequencies and related impact on characteristics of chaos;
- (c) Potential applications for another two-level finite-lattice class of models with localization-delocalization phase transition, e.g., in (i) ultracold Bose gas in optical lattices: The Bose-Einstein condensation exhibits the phase coherence of Bose atoms destroyed by the suppression of the tunneling due to the localization by the strong lattice potential [24, 25]; (ii) recently discovered Bose-Einstein condensation of exciton polaritons (bosons), coupled light-matter bosonic quasiparticles [15] in semiconductor microcavities. Theoretical investigation of the phase transition to the polariton condensation state, including finite-size fluctuations and quantum effects vs finite temperatures were reported [7, 16, 18]. The finite-size effects for the polariton condensation phase transition within the Dicke model were studied by Eastham et al [16] and scaling corrections to the critical exponents for the Dicke model at the crossover were studied by Vidal et al [26].

The finite-size aspect appears naturally in our system through two kinds of fluctuations:

1. Finite-size fluctuations in *electron* subsystem due to the finiteness of the lattice and  
 2. fluctuations in *boson* subsystem – level spacing fluctuations in the discrete set of excited levels of the boson spectra. The signs of complexity are the multiple quantum level repulsions and respective level avoidings. They interplay with quantum correlations and are responsible for the spectral characteristics with the signatures of quantum chaos. The quantum correlations competing the level repulsions include (i) mode selfinteraction (squeezing) resulting in reduction of the mode frequency and stabilizing the ground state. (ii) Quantum correlations between two different modes (entanglement). The two-boson (squeezed) coherent states are analogous to the squeezed coherent states in quantum optics introduced by Yuen [27].

(The fluctuations due to the discreteness of spectra even without the signs of complexity are known to be present in a number of coupled quantum electron-phonon systems that do not admit the use of the adiabatic approximation [28]. They cause smooth crossover in localization-delocalization phase transition not accompanied by a non-analytical change of the ground state).

In Section II we define the model under investigation and review the representation of the Dicke multispin collective states. In Section III we investigate numerically and analytically the ground state. For analytical calculations we use the Holstein-Primakoff bosonisation Ansatz for the multispin operators. In Section IV we present an approximate analytical investigation of the role of nonlinear terms accompanying the finite-size effects. It provides a useful, though approximate, insight into a scenario of interaction of three effective oscillators especially on a formation of the mixed phase.

In Section V, after a brief summary of realms of the theory of quantum spectral chaos, we show numerical results on statistical signatures of the quantum chaos - the probability distributions of nearest neighbour level spacings (NNLS), spectral entropies and spectral densities for different numbers of lattice sites, frequencies and coupling parameters. The interference of the finite-size fluctuations in electron space with boson level spacing fluctuations will be demonstrated by the statistical characteristics implying the quantum chaotic behaviour. A qualitative difference between the present model and the one-boson Dicke model will be illustrated by comparison of the nearest NNLS distributions of both models.

Considering possible applications, in Conclusion we propose several interpretations of experimental results. Generally, the concepts of the model above can be applied for nanostructures where the quantum effects are found rather detectable [29].

## 2. Model

We consider a finite lattice array of localized JT molecules - two electron levels at each lattice site dipole- coupled to two vibron modes of different symmetry against reflection with different coupling strengths and different frequencies. The simplest (one-boson)  $E \otimes \beta$  version of the JT model, in the collective coordinate approximation, reveals a formal analogy to the one-boson Dicke model [5] or to the exciton or dimer model.

The JT Hamiltonian generalized to multiple dimensionality of the (pseudo)spin space and different boson frequencies is of the form

$$H = (\Omega_1 a_1^\dagger a_1 + \Omega_2 a_2^\dagger a_2) I + \frac{1}{\sqrt{N}} \sum_{i=1}^N \left[ \alpha (a_{1i}^\dagger + a_{1i}) 2s_z^{(i)} + \beta (a_{2i}^\dagger + a_{2i}) (s_+^{(i)} + s_-^{(i)}) \right]. \quad (1)$$

The wave functions of the localized JT molecules do not overlap. The bosons represent intramolecular vibrons: the antisymmetric against reflection mode  $\Omega_1$ ,  $a_1$  assists the splitting of the level (in the Dicke model the level separation is a model parameter). The symmetric boson mode  $a_2$  assists the tunneling between the levels. (Evidently, the simplest one boson version of the JT model ( $E \otimes \beta$ ) and the Dicke model are related by a unitary transformation - rotation in the pseudospin  $2 \times 2$  space). The dipole electron-boson coupling causes the non-conservation of the coherent bosons number and, consequently, implies the nonintegrability of Hamiltonian (1) as opposed to the Jaynes-Cummings model.

The on-site displacements are homogeneous along the lattice: The sites (levels) are equally displaced within the  $N = 2j$  multiplicity, so that we can omit the index  $i$  of the dipole momentum operator in (1). Then, using the Dicke collective ( $N$ -dimensional) spin variables  $J_z = \sum_i s_z^{(i)}$ ,  $J_+ = \sum_i s_+^{(i)}$ ,  $J_- = \sum_i s_-^{(i)}$ , Hamiltonian (1) can be rewritten to the Dicke-like form

$$H = (\Omega_1 a_1^\dagger a_1 + \Omega_2 a_2^\dagger a_2) I + \frac{\alpha}{\sqrt{2j}} (a_1^\dagger + a_1) \cdot 2J_z + \frac{\beta}{\sqrt{2j}} (a_2^\dagger + a_2) (J_+ + J_-). \quad (2)$$

The operators  $J_\pm$ ,  $J_z$  satisfy the same commutation relations as the individual spins:

$$[J_z, J_\pm] = \pm J_\pm; \quad [J_+, J_-] = 2J_z \quad (3)$$

where  $J_x = \frac{1}{2}(J_+ + J_-)$ ,  $J_y = -\frac{i}{2}(J_+ - J_-)$ .

The scaling by  $1/\sqrt{2j}$  in (2) accounts for lengths of the dipoles  $2j = 1, 2, \dots, N$ . It was chosen equal for both interaction terms for symmetry, but eventual rescaling of one of the coupling constants  $\alpha$ ,  $\beta$  is evidently possible, if necessary.

The model (2) can be also considered as a generalization of one-boson Dicke model

$$H_D = \Omega a^\dagger a I + \omega_0 J_z + \frac{\lambda}{\sqrt{2j}} (a^\dagger + a) (J_+ + J_-). \quad (4)$$

### 2.1. Representation of the Dicke states

The Dicke states are represented by the spin operators of higher dimensions [5]. Each Dicke state is labeled as  $|j, m\rangle$  with the discrete index  $m$  ranging (at fixed  $j$ ) from  $-j, -j+1, \dots$  to  $j$ . The spin operators in the Dicke space are defined as follows:

$$\begin{aligned} J_z |j, m\rangle &= m |j, m\rangle; \quad J_\pm |j, m\rangle = \sqrt{j(j+1) - m(m \pm 1)} |j, m \pm 1\rangle; \\ J^2 |j, m\rangle &= j(j+1) |j, m\rangle. \end{aligned} \quad (5)$$

The subspaces  $j$  are independent and, hence, one can consider them separately keeping  $j$  fixed. For the chain containing  $N$  atoms possible values of  $j$  range as

$0, 1, \dots, N/2$  for  $N$  even and  $1/2, 3/2, \dots, N/2$  for  $N$  odd; for given  $j$  the operators  $J_i$  are matrices with dimensions  $2j + 1$  (representations of the  $SU(2)$  group). In what follows we shall always take into consideration only the subspace with largest  $j = N/2$  for each number of atoms in a chain.

The operator of parity  $\Pi = \exp\{i\pi(a_i^\dagger a_i + J_z + j)\}$ ,  $i = 1, 2$  commutes with Hamiltonian (4). For the JT molecule with only two electron levels ( $j = 1/2$ ) and equal boson frequencies this fact reflects itself in the conserved parity  $p = \pm 1$  [30, 21] as an additional good quantum number. For parities  $+1$  and  $-1$  the spectra of that model are identical. As we shall see, for the present generalization this is the case of even number of molecules, that is for the main Dicke numbers  $j = 1/2, 3/2, \dots$

### 3. Ground state

The method of collective pseudospin variables provides a useful insight into the scenario of the interplay of interactions in the system of three effective oscillators. The Holstein-Primakoff Ansatz [36] for the collective pseudospin operators (3) reads

$$J_z = b^\dagger b - j, \quad J_+ = b^\dagger \sqrt{2j - b^\dagger b}, \quad J_- = \sqrt{2j - b^\dagger b} b. \quad (6)$$

Here  $b$  are fictitious boson operators which satisfy boson commutation rules  $[b, b^\dagger] = 1$ ; this representation of the spin algebra preserves exactly the commutation relations (3) and makes it possible to convert the system to two or three coupled quantum oscillators as will be shown below. (Let us remark that the Holstein-Primakoff Ansatz (6) breaks the symmetry of Hamiltonian (2) with respect to a simultaneous exchange of  $\alpha \leftrightarrow \beta$ ,  $\Omega_1 \leftrightarrow \Omega_2$  and  $J_z \leftrightarrow J_x = J_+ + J_-$  well known for the Jahn-Teller model with  $2j = 1$ .)

Linear terms in Hamiltonian (2) can be excluded by use of the coherent state representation with boson displacements chosen variationally providing  $\langle b^\dagger b \rangle / 2j \ll 1$ , i.e. close to saturation [36]. Let us displace the operators involved as follows

$$a_1^\dagger = c_1^\dagger + \sqrt{\alpha_1}, \quad a_2^\dagger = c_2^\dagger + \sqrt{\alpha_2}, \quad b^\dagger = d^\dagger - \sqrt{\delta}. \quad (7)$$

Applying the Holstein-Primakoff Ansatz (6), setting (7) into (2) and expanding the square root expressions in (6) yields the form

$$\begin{aligned} H \approx & \Omega_1 (c_1^\dagger c_1 + 1/2) + \Omega_2 (c_2^\dagger c_2 + 1/2) + \Omega_1 \alpha_1 + \Omega_2 \alpha_2 + \Omega_1 \sqrt{\alpha_1} (c_1^\dagger + c_1) \\ & + \Omega_2 \sqrt{\alpha_2} (c_2^\dagger + c_2) + \frac{2\alpha}{\sqrt{2j}} [(c_1^\dagger + c_1) d^\dagger d + 2\sqrt{\alpha_1} d^\dagger d - \sqrt{\delta} (c_1^\dagger + c_1)(d^\dagger + d) \\ & - 2\sqrt{\alpha_1} \delta (d^\dagger + d) + (\delta - j)(c_1^\dagger + c_1) + 2\sqrt{\alpha_1}(\delta - j)] \\ & + \frac{\beta}{\sqrt{2j}} (c_2^\dagger + c_2 + 2\sqrt{\alpha_2}) \cdot k \left\{ -2\sqrt{\delta} + (1 - \delta/k^2)(d^\dagger + d) + \frac{\sqrt{\delta}}{k^2} d^\dagger d \right. \\ & \left. + \frac{1}{2k^2} [-(d^{\dagger 2} d + d^\dagger d^2) + \sqrt{\delta}((d^\dagger + d)^2 - 1)] \right\}, \quad k \equiv \sqrt{2j - \delta}. \end{aligned} \quad (8)$$

From the condition of elimination of the terms linear in boson operators from (8) three identities for the parameters  $\alpha_i$  and  $\delta$  follow ( $k \neq 0$ ):

$$\begin{aligned}\Omega_1 \sqrt{\alpha_1} &= -\frac{2\alpha}{\sqrt{2j}}(\delta - j), \\ \Omega_2 \sqrt{\alpha_2} &= \frac{\beta\sqrt{\delta}}{\sqrt{2j}} \frac{4j - 2\delta + 1/2}{\sqrt{2j - \delta}}, \\ \sqrt{\delta}(\delta - j) \left( 4\Omega_2 \alpha^2 - 2\Omega_1 \beta^2 \frac{4j - 2\delta + 1/2}{2j - \delta} \right) &= 0.\end{aligned}\tag{9}$$

For finite  $j$ , this set of equations implies three solutions provided  $\Omega_2 \alpha^2 \neq \Omega_1 \beta^2(1 + 1/8j)$  as follows:

$$\sqrt{\alpha_1} = \frac{\alpha}{\Omega_1} \sqrt{2j}, \quad \alpha_2 = 0, \quad \delta = 0 \tag{10a}$$

$$\alpha_1 = 0, \quad \sqrt{\alpha_2} = \frac{\beta}{\Omega_2} \sqrt{2j} \left( 1 + \frac{1}{4j} \right), \quad \delta = j, \tag{10b}$$

$$\sqrt{\alpha_1} = -\frac{\alpha}{\Omega_1} \sqrt{2j(1 - 2\bar{\mu})}, \quad \sqrt{\alpha_2} = \frac{2\alpha^2}{\Omega_1 \beta} \sqrt{2j\bar{\mu}(1 - \bar{\mu})}, \quad \delta = 2j(1 - \bar{\mu}), \tag{10c}$$

where in (10c)  $\bar{\mu} = \frac{\bar{\beta}^2}{8j(\alpha^2 - \bar{\beta}^2)} < 1$ , and  $\alpha > \bar{\beta} \equiv \sqrt{\Omega_1/\Omega_2} \beta$ .

The first two solutions are similar to that reported for the Dicke model of superradiance [8, 9, 11, 37] in the limit  $j \rightarrow \infty$ , so that in this limit they account for the common normal and super-radiant phases. In this case the condition  $\alpha\sqrt{\Omega_2} = \beta\sqrt{\Omega_1}$  would represent the point of the quantum phase transition. The phase transition for the present model means transition from the state (10a) with zero macroscopic occupation to the fully excited  $q$ -bit state (10b). In the semiclassical limit this would imply possible concept of a "superradiant phonon state" (10b).

On the other hand, for finite  $j$ , third solution (10c) represents specific finite-size effects; the thermodynamic limit (and thus the phase transition) is forbidden due to the condition  $0 < \bar{\mu} < 1$ . Instead of the phase transition between the normal (10a) and radiation (10b) phase, there appears a crossover (intermediate) domain within the "normal" domain (10c). In this case all three oscillators are coupled: the parameter  $\bar{\mu}$  (10c) is a measure of the coupling. Evidently, in the limit  $j \rightarrow \infty$  the phase (10c) vanishes.

### 3.1. Case 1: Polaron self-trapping in the normal domain

In this case (10a) we expect an impact of the additional oscillator  $a_1$  (here its fluctuations  $c_1$  (7)) on the behaviour of the normal phase.

The solution (10a) represents the normal phase with average zero number of macroscopically excited electron level bosons  $\delta = 0$ . Hamiltonian (8) related to this solution reads

$$H_1 = \Omega_1 (c_1^\dagger c_1 + 1/2) + \Omega_2 (c_2^\dagger c_2 + 1/2) + \frac{4\alpha^2}{\Omega_1} (d^\dagger d - j/2) + \beta (c_2^\dagger + c_2)(d^\dagger + d)$$

$$+\frac{2\alpha}{\sqrt{2j}}(c_1^\dagger + c_1)d^\dagger d - \frac{\beta}{4j}(c_2^\dagger + c_2)(d^{\dagger 2}d + d^\dagger d^2). \quad (11)$$

Here, the level oscillator acquires the frequency of a polaron-dressed oscillator  $\omega_1 = 4\alpha^2/\Omega_1$  which results from the self-trapping by the additional mode in contrast with respective factor of the Dicke model  $\omega_0$ . Explicit interaction of the oscillator modes with the level bosons contribute only to excited states  $\sim 1/\sqrt{j}$  in (11). For large  $j$  only linear terms persist (first line in (11)) and Hamiltonian (11) can be easily diagonalized by a rotation in the plane of coupled operators  $c_2$  and  $d$  [9] to yield the form

$$H_{1d} = \Omega_1 c_1^\dagger c_1 + \epsilon_{1,+} C_2^\dagger C_2 + \epsilon_{1,-} C_3^\dagger C_3 - 2\alpha^2 j / \Omega_1 \quad (12)$$

with new effective oscillators  $C_2, C_3$ . The excitation energies of the system  $\epsilon_{1,\pm}$  in the thermodynamic limit are

$$\epsilon_{1,\pm}^2 = \frac{1}{2} \left( \Omega_2^2 + \omega_1^2 \pm \left[ (\Omega_2^2 - \omega_1^2)^2 + 64\alpha^2 \beta^2 \Omega_2 / \Omega_1 \right]^{1/2} \right). \quad (13)$$

From (13), the solution for  $\epsilon_1$  exists provided  $\omega_1 > 4\beta^2/\Omega_2 \equiv \omega_2$ , or if  $\alpha\sqrt{\Omega_2} > \beta\sqrt{\Omega_1}$ . This phase is identified as the normal phase of the Dicke-like model without macroscopic excitations, Figure 1. The effect of different initial frequencies  $\Omega_1 \neq \Omega_2$  is just the shift of the phase transition point supporting the phase with the smaller of  $\Omega_i$ .

From (11), critical Hamiltonian  $H_1^{crit} = H_1(\beta_c = \alpha\sqrt{\Omega_2/\Omega_1})$  at the point of the phase transition yields

$$H_1^{crit} = \sqrt{\Omega_2^2 + (4\alpha^2/\Omega_1)^2} (C_2^\dagger C_2 + 1/2) + \Omega_1 (c_1^\dagger c_1 + 1/2) - 2\alpha^2 j / \Omega_1. \quad (14)$$

The coupled undisplaced oscillators  $a_2$  and  $d$  form an effective single oscillator of the frequency  $\sqrt{\Omega_2^2 + (4\alpha^2/\Omega_1)^2}$ . The mixing results from the coupling due to the assisting oscillator  $a_2$  between the levels split by the oscillator  $a_1$ .

### 3.2. Case 2: Squeezing in the radiation domain.

The second solution (10b) identified further with the radiation domain, can be treated on the same footing. For this solution the level bosons (6) are displaced by  $\delta = j$  which represents the number of excited states within the domain. Respective Hamiltonian (8) yields

$$H_2 = H_2^{(1)} + H_2^{(2)}, \quad (15)$$

where

$$\begin{aligned} H_2^{(1)} &= \Omega_1 (c_1^\dagger c_1 + 1/2) + \Omega_2 (c_2^\dagger c_2 + 1/2) + 4\beta^2 (1 + 1/4j) d^\dagger d / \Omega_2 \\ &- \sqrt{2}\alpha (c_1^\dagger + c_1)(d^\dagger + d) + \beta^2 (1 + 1/4j) (d^{\dagger 2} + d^2) / \Omega_2, \end{aligned} \quad (16)$$

and a fluctuation part of nonlinear interaction terms  $O(1/\sqrt{j})$ ,  $O(1/j)$ ,

$$\begin{aligned} H_2^{(2)} &= \frac{1}{\sqrt{2j}} \left( 2\alpha (c_1^\dagger + c_1) d^\dagger d + \beta (c_2^\dagger + c_2) d^\dagger d + \beta (c_2^\dagger + c_2) [(d^\dagger + d)^2 \right. \\ &\left. - (d^{\dagger 2}d + d^\dagger d^2) / \sqrt{j}] / 2 - \sqrt{2}\beta^2 (1 + 1/4j) (d^{\dagger 2}d + d^\dagger d^2) / \Omega_2 \right). \end{aligned} \quad (17)$$



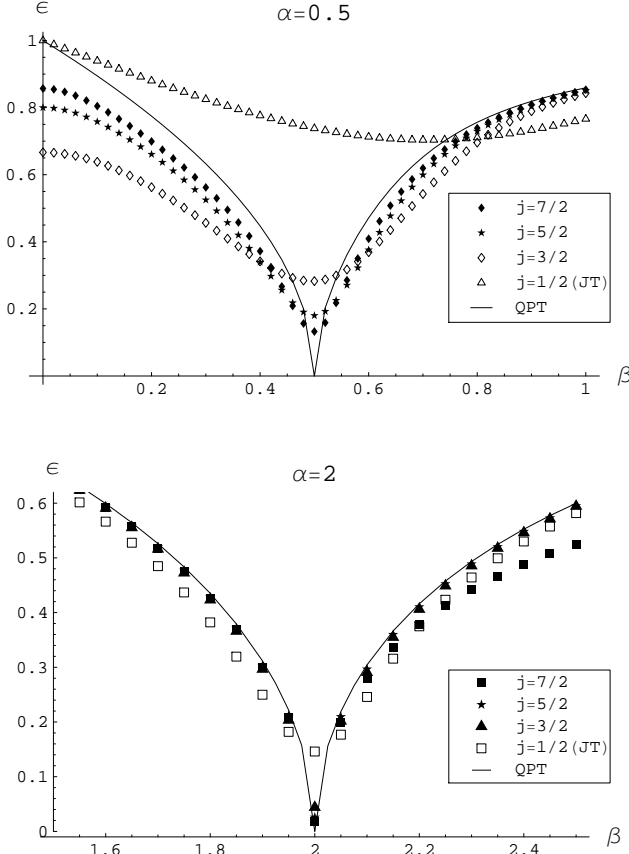


**Figure 1.** Crossover between the normal and radiation domain in the generalized JT lattice model for  $\alpha = 0.5, 2$  and resonance case  $\Omega_1 = \Omega_2 = 1$ . The numerical results for the excitation energy of the first excited state for different  $j$  are shown, the solid line in each figure is the analytical result for asymptotic QPT (13), (21) valid for  $j \rightarrow \infty$ . The cusp-like behavior close to the point of the crossover  $\omega_1 \equiv 4\alpha^2/\Omega_1 = 4\beta^2/\Omega_2^2 \equiv \omega_2$  appears already for relatively small number of sites, e.g., for  $j = 7/2$ . For small  $j$ , the fluctuations smooth the cusp especially at weak couplings. The non-symmetry about the critical point by the reduction of the energy in the radiation domain for  $\alpha = 0.5$  is due to the squeezing. For the case of different  $\Omega_1 \neq \Omega_2$  the picture is qualitatively the same, there occurs a shift of the transition inwards the phase with higher  $\Omega_i$ .

In Hamiltonian (16), the level polaron is linearly coupled with the oscillator 1. The nonlinear selfinteracting term  $\sim d^{\dagger 2} + d^2$  can be transformed out by the unitary operator  $S = \exp[r(d^{\dagger 2} - d^2)]$  using the identities

$$\begin{aligned} \tilde{d}^{\dagger} \tilde{d} &\equiv S^{-1} d^{\dagger} d S = d^{\dagger} d \cosh 4r + \sinh^2 2r + (d^2 + d^{\dagger 2}) \frac{1}{2} \sinh 4r, \\ (\tilde{d}^{\dagger} + \tilde{d}) &\equiv S^{-1} (d^{\dagger} + d) S = (d^{\dagger} + d) e^{-2r}. \end{aligned} \quad (18)$$

By comparing (16) and (18) one obtains selfconsistently the renormalized frequency  $\omega_2 = \frac{4\beta^2}{\Omega_2 \cosh 4r} (1 + 1/4j)$  and the interaction parameter  $\kappa = \sqrt{2}\alpha e^{2r}$ . The value of the squeezing parameter  $r$  is given by  $\tanh(4r) = 2\beta^2/\Omega_2^2$ . Up to the terms of the order  $j^0$  we get

$$\begin{aligned} \tilde{H}_2^{(1)} &\equiv S H_2^{(1)} S^{-1} = \Omega_1 (c_1^{\dagger} c_1 + 1/2) + \Omega_2 (c_2^{\dagger} c_2 + 1/2) + \omega_2 \tilde{d}^{\dagger} \tilde{d} \\ &\quad - \kappa (c_1^{\dagger} + c_1) (\tilde{d}^{\dagger} + \tilde{d}) - 4\beta^2 \sinh^2 2r / \Omega_2. \end{aligned} \quad (19)$$



As a result, the quantum fluctuations  $\sim d^{\dagger 2} + d^2$  renormalize the frequency  $\Omega_2 \rightarrow \omega_2$ , interaction  $\alpha \rightarrow \kappa$  and the ground state (19).

Diagonalization of (19) results in three effective independent oscillators  $C_1, C_3$  and  $c_2$ , the last one remaining free,

$$H_{2d} = \epsilon_{2,+} C_3^\dagger C_3 + \epsilon_{2,-} C_1^\dagger C_1 + \Omega_2 c_2^\dagger c_2 - 4\beta^2 \sinh^2 2r / \Omega_2 + (\Omega_1 + \Omega_2) / 2, \quad (20)$$

where

$$\epsilon_{2,\pm}^2 = \frac{1}{2} \left( \Omega_1^2 + \omega_2^2 \pm [(\Omega_1^2 - \omega_2^2)^2 + 64\alpha^2 \beta^2 e^{4r} \Omega_1 / \Omega_2]^{1/2} \right). \quad (21)$$

From (21) one obtains the condition for stability of the linear phase

$$\beta^2 / \Omega_2 > \alpha^2 e^{4r} / \Omega_1. \quad (22)$$

From (22) we receive the nonsymmetry of the radiation vs. the "normal" domain due to the squeezing: suppression of the radiation domain. The non-symmetry of both branches of the excitation energy is also evident from the numerical results in Figure 1 from the exact Hamiltonian (1).

The analysis of both domains shows that within linear approximation the oscillator  $c_1$  in the radiation domain plays qualitatively the same role as does the oscillator  $c_2$  in the normal domain with simultaneous interchange of the polaron frequencies  $\omega_1 \leftrightarrow \omega_2$  and coupling constants  $\alpha\sqrt{\Omega_2} \leftrightarrow \beta\sqrt{\Omega_1}$ . Hence, in linear approximation two of the oscillators mix to two-dimensional effective oscillator while the remaining one is decoupled. Linear analysis in adiabatic approximation of subsections 3.1 and 3.2 yields an *acoustic analogue* of the Dicke phase transition between the normal and super-radiant phases.

### 3.3. Case 3. Intermediate domain of mixed "quasi-normal" and "radiation" domains

A qualitatively new situation occurs in the nonlinear regime at finite  $j$ , when all three oscillators couple via interplay of fluctuations due to finite  $j$ . This situation is represented by the solution (10c). This solution yields for Hamiltonian (8)

$$\begin{aligned} H_3 = & \Omega_1 (c_1^\dagger c_1 + 1/2) + \Omega_2 (c_2^\dagger c_2 + 1/2) + \frac{4\alpha^2 \bar{\mu}}{\Omega_1} d^\dagger d + \frac{2\alpha^2}{\Omega_1} (1 - \bar{\mu}) (d^\dagger + d)^2 \\ & - 2\alpha \sqrt{1 - \bar{\mu}} (c_1^\dagger + c_1) (d^\dagger + d) + \beta \frac{2\bar{\mu} - 1}{\sqrt{\bar{\mu}}} (c_2^\dagger + c_2) (d^\dagger + d) \\ & + \frac{1}{\sqrt{2j}} \left[ 2\alpha (c_1^\dagger + c_1) d^\dagger d + \beta \frac{\sqrt{1 - \bar{\mu}}}{2\sqrt{\bar{\mu}}} (c_2^\dagger + c_2) d^\dagger d + \frac{\beta}{2} \frac{\sqrt{1 - \bar{\mu}}}{\sqrt{\bar{\mu}}} (c_2^\dagger + c_2) (d^\dagger + d)^2 \right. \\ & \left. - \frac{2\alpha^2}{\Omega_1} (1 - \bar{\mu})^{1/2} (d^{\dagger 2} d + d^\dagger d^2) - \frac{\beta}{2\sqrt{2j}\sqrt{\bar{\mu}}} (c_2^\dagger + c_2) (d^{\dagger 2} d + d^\dagger d^2) \right] \\ & - \frac{2\alpha^2}{\Omega_1} j (1 + 4\bar{\mu}(1 - \bar{\mu})) + \frac{8\alpha^4 \Omega_2 j}{\beta^2 \Omega_1^2} \bar{\mu} (1 - \bar{\mu}) - \frac{2\alpha^2 (1 - \bar{\mu})}{\Omega_1}, \end{aligned} \quad (23)$$

where  $\bar{\mu} = \frac{\beta^2 \Omega_1}{8j(\alpha^2 \Omega_2 - \beta^2 \Omega_1)} < 1$ ,  $\alpha > \beta \sqrt{\frac{\Omega_1}{\Omega_2}} \equiv \bar{\beta}$ .

Hamiltonian (23) implies a complex nonlinear interplay of the quantum oscillators. The dressing of all oscillators due to the finite  $j$  is evident; for example, for the level

boson  $d$  its effective frequency can be estimated by approximate quasiclassical analysis as  $\omega = \frac{4\alpha^2}{\Omega_1} \left(1 - \frac{\beta^2 \Omega_1}{\alpha^2 \Omega_2}\right)^{1/2} |(1 - 2\bar{\mu})|$ .

In the intermediate quantum domain between the quasi-normal and the reduced radiation domain, three polarons, the dressed level boson  $d$ , the dressed bosons 1 and 2 mix due to the finite-size fluctuations.

Numerical evaluation of the order parameter  $J_z$  from the exact Hamiltonian (1) in Figure 2 illustrates the existence of the intermediate phase as a partial occupation of the radiation domain in the neighborhood of the point  $\alpha = \bar{\beta}$  even within the normal domain  $\alpha > \bar{\beta}$ . The difference of frequencies  $\Omega_1 \neq \Omega_2$  only renormalizes the position of the asymptotic transition point in Figures 1, 2 by broadening the domain of the smaller frequency: the transition point shifted inwards the domain with larger  $\Omega_i$ .

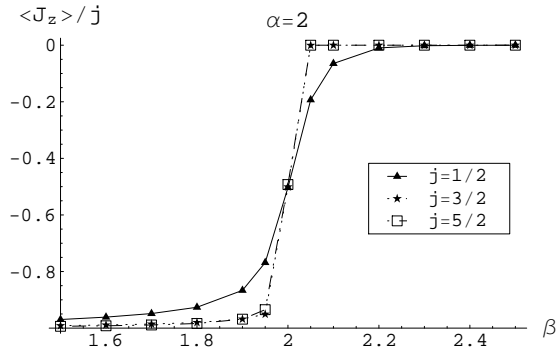


**Figure 2.** Order parameter  $\langle J_z \rangle / j$  for  $j = 1/2, 3/2, 5/2$  and  $\Omega_1 = \Omega_2$ . The finite-size effect ( $j$  finite) of the mixed domain about the crossover vanishes asymptotically for  $j \rightarrow \infty$ .

#### 4. The symmetry breaking by semiclassical approach

Linear analysis of the previous section enabled us to investigate each of the domains separately. As the next step, in (8) we include small nonlinear terms up to  $O(1/j)$  to explore the finite-size effects.

Heisenberg equations related to (11) for the case 1 read as follows

$$\begin{aligned} i\dot{c}_1 &= \Omega_1 c_1 + \frac{2\alpha}{\sqrt{2j}} d^\dagger d, & i\dot{c}_2 &= \Omega_2 c_2 + \beta(d^\dagger + d) - \frac{\beta}{4j}(d^{\dagger 2} d + d^\dagger d^2), \\ i\dot{d} &= \frac{4\alpha^2}{\Omega_1} d + \frac{2\alpha}{\sqrt{2j}}(c_1^\dagger + c_1)d + \beta(c_2^\dagger + c_2) - \frac{\beta}{4j}(c_2^\dagger + c_2)(2d^\dagger d + d^2). \end{aligned} \quad (24)$$

For strong interaction it is plausible to assume  $\omega_1 = \frac{4\alpha^2}{\Omega_1} \gg \Omega_1, \Omega_2$ . Then, we can apply the adiabatic approximation neglecting intrinsic dynamics of the level polaron  $d$  of high frequency  $\omega_1$ ,  $\dot{d} = 0$ . Consequently, it can be eliminated, so that it influences only implicitly the dynamics of the modes  $q_1 = (2\Omega_1)^{-1/2} \langle c_1^\dagger + c_1 \rangle$  and  $q_2 = (2\Omega_2)^{-1/2} \langle c_2^\dagger + c_2 \rangle$ . We can use the stationary expression for  $q = (8\alpha^2/\Omega_1)^{-1/2} \langle d^\dagger + d \rangle$  from (24). Then, the dynamic equations for  $q_1$  and  $q_2$ , up to the lowest order term in  $1/\sqrt{j}$  read

$$\ddot{q}_1 = -\Omega_1^2 q_1 - \frac{\beta^2 \Omega_1 \sqrt{\Omega_1} \Omega_2}{4\alpha^3 \sqrt{j}} q_2^2, \quad (25)$$

$$\ddot{q}_2 = -\Omega_c^2 q_2 - \frac{\beta^2 \Omega_1^2 \sqrt{\Omega_1}}{\alpha^3 \sqrt{2j}} q_1 q_2, \quad (26)$$

where  $\Omega_c = \Omega_2 (1 - \bar{\beta}^2/\alpha^2)^{1/2}$ , ( $\alpha > \bar{\beta}$ ).

We received effectively softened frequency of the oscillator  $q_2$  which justifies again the use of the slaving principle for the oscillator  $q_1$ ,  $\Omega_1^2 \gg \Omega_1^2(1 - \bar{\beta}^2/\alpha^2)$ . Its dynamics is then implicitly ordered by the dynamics of the oscillator  $q_1$ . Then, similarly as in the previous case, we obtain

$$\ddot{q}_2 = -\frac{dV(q_2)}{dq_2}, \quad (27)$$

where

$$V(q_2) = \frac{1}{2} \Omega_c^2 q_2^2 + \frac{\beta^5 \Omega_1^2 \Omega_2}{16 \alpha^6 j \sqrt{2}} q_2^4 + V_0. \quad (28)$$

Thus, for finite  $j$ , equation (27) for the fluctuations  $q_2$  in the normal domain represents the ideal Duffing oscillator. The potential (28) implies a stable "normal" phase up to the condition  $\alpha = \bar{\beta} \equiv \beta \sqrt{\Omega_1/\Omega_2}$  to the order  $1/j$  for each  $j$ .

We conclude that in the adiabatic approach in the normal domain there occur finite-size fluctuations and instability of the oscillator (26) because of softening its frequency  $\bar{\omega}_2$ ; the softening here represents approaching closer the radiation domain.

Let us suppose that the energies at both sides of the transition between the normal and the radiation domains are symmetric when interchanging  $\alpha \leftrightarrow \beta$  and  $\Omega_1 \leftrightarrow \Omega_2$ , ( $r \rightarrow 0$ ). In the radiation domain the nonlinearity yields one-instanton solution

$$\bar{q}_{21}(\tau - \tau_0) = \pm \frac{2\alpha_1^3}{\beta^2 \Omega_1} \left[ \frac{2j}{\Omega_1} (1 - \alpha^2/\bar{\beta}^2) \right]^{1/2} \tanh \left( \frac{\Omega_1}{\sqrt{2}} (1 - \alpha^2/\bar{\beta}^2)^{1/2} (\tau - \tau_0) \right). \quad (29)$$

Here,  $\bar{q}_2 = q_2 \sqrt{\Omega_1/\Omega_2}$ ,  $\bar{\beta} = \beta \sqrt{\Omega_1/\Omega_2}$ . The one-instanton solution (29) is associated with the tunneling between the extrema of the potential inverted to (28) if  $\bar{\beta} > \alpha$  and  $\tau \rightarrow it$ . Hence, at finite  $j$ 's there appears new instanton phase at the maximum softening of the frequency at  $\bar{\beta} \rightarrow \alpha$  in the radiation domain. Generally, there occurs a sequence of repeated tunnelings (oscillations between two equivalent minima of a local potential) for each lattice site. Moreover, there exists the coupling between the oscillators 1 and 2 (25, 26) which was neglected in the linear approximation (27). In fact, within more subtle calculations there would occur tunnelings mediated by two coupled oscillators (one of them being a polaron) for each  $j$  instead of one of the adiabatic treatment.

## 5. Statistical characteristics for excited boson complex spectra

For  $\alpha = 0$  or  $\beta = 0$ , the excited boson spectrum of the Hamiltonian (1) is the superposition of two sets of levels of Fock harmonic oscillators. If  $\alpha \neq \beta \neq 0$ , respective wave functions of excited states become to overlap and the nearest levels strongly repulse which results in multiple level-avoidings. The spectrum acquires respective degree of complexity, i.e., of quantum chaotic behaviour. For the excited complex spectra of

atoms, molecules and nuclei [14, 19], several spectral characteristics as signatures of quantum chaos were introduced. The mostly used one is the probability distribution function  $P(S)$  of the nearest-neighbour level spacings (NNLS) utilized as a standard testing point for investigation of the issues in spectral quantum chaology [14]. The excited spectra of a supposedly quantum chaotic system can be modeled in terms of statistical ensembles for which the random matrix theory specifies several classes of universal probability distributions (Wigner surmise) of the NNLS dependent solely on the symmetry of the underlying Hamiltonians [19]. In the case of the Dicke model the NNLS distribution is namely the Wigner-Dyson one  $P(S) \sim S \exp(-S^2)$  which is the sign of fully developed quantum chaos [9, 19]. In the absence of overlapping of the wave functions, respective levels become to cross each other and the Poisson distributions  $P(S) \sim \exp(-S)$  result.

Recently we have reported the results on NNLS distribution for excited boson spectrum of the JT model (taken as function of coupling constants  $\alpha, \beta$ ) [22, 38] which is the case  $j = 1/2$ ,  $\Omega_1 = \Omega_2$ ,  $\alpha \neq \beta$  in the notation of (2) of the present paper. These distributions essentially deviate from the prediction of the Wigner-Dyson form. The peculiarity of the JT system of a single molecule with equal frequencies was that the Wigner-Dyson distribution for  $P(S)$  has never been reached, but the distribution close to the semi-Poisson form  $P(S) = 4S \exp(-2S)$  appeared as the most typical “chaotic” one.

In this section we present statistical characteristics (NNLS distributions, entropy of level occupation and spectral density of states) for  $\Omega_1 \neq \Omega_2$ ,  $j \geq 1/2$ . We solved numerically the eigenvalue problem for quantum Hamiltonian (1). This Hamiltonian was diagonalized with the basis of the boson Fock states for bosons 1 and 2. An inevitable truncation error was produced when taking only  $N_1$  and  $N_2$  boson Fock states for each of  $2j + 1$  electron levels, so that the results were checked against the convergence (with changing the numbers  $N_1, N_2$ ). Only about  $\sim 1100$  lower states were used for calculation of the statistics out of typically  $\sim (8 \div 10) \times 10^3$ . The raw energy spectrum obtained had to be treated by an unfolding procedure in order to ensure the homogeneity of the spectrum (constant local density of levels). Thereafter the statistical data were gathered in a standard fashion from small intervals in the space of parameters  $(\alpha, \beta)$ . The calculations were performed essentially along the same lines as our previous calculations for the Jahn-Teller problem with  $j = 1/2$  [22, 38] where additional details are given as to the convergence check, unfolding procedure and gathering statistics.

The results for the level spacing distributions for different phonon frequencies  $\Omega_1 \neq \Omega_2$  and  $j > 1/2$  show rather vast variety ranging from the Wigner-Dyson to the Poisson distribution as limiting cases but recovering also the semi-Poisson distribution in a rather wide range of model parameters. With increasing  $j$ , general tendency consists in increasing the range of parameters where the NNLS shows deviations from the Poisson form towards chaoticity up to its maximum degree of the Wigner-Dyson form. For moderate  $j$  ( $j = 7/2$  and  $\Omega_1 \neq \Omega_2$  exemplified in Figure 3) there appears a well-marked domain of the Wigner-Dyson distribution. For example, for  $\Omega_2/\Omega_1 = 2$  this domain

stretches for the values of parameters  $1 < \alpha, \beta < 3$ .

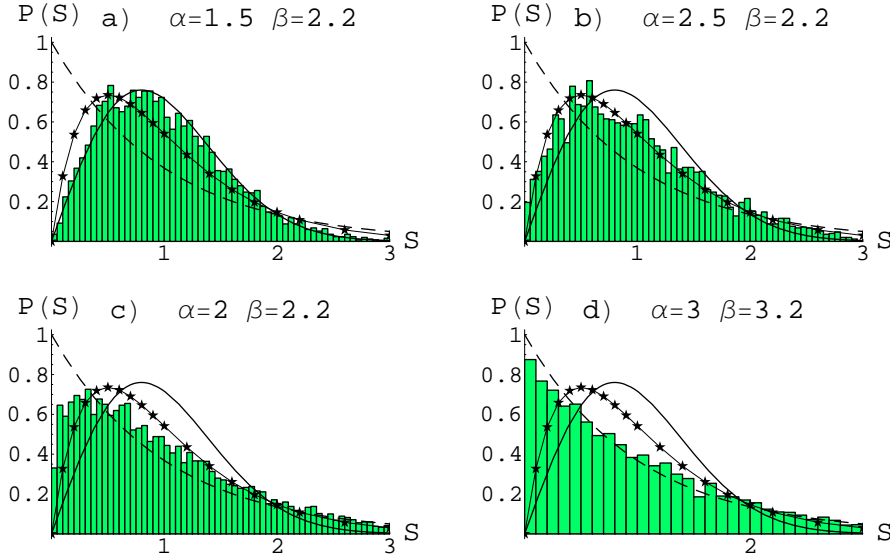


**Figure 3.** Level spacing distributions for  $j = 7/2$  and different  $(\alpha, \beta)$  (parameters are scaled to  $\Omega_1 = 1$ ). Upper row ((a,b)):  $\Omega_2 = 2\Omega_1$ ; bottom row ((c,d)):  $\Omega_2 = 0.5\Omega_1$ . The curves show Wigner-Dyson (solid), Poisson (dashed) and semi-Poisson (stars) distributions. NNLS distributions in b), c) are close to the semi-Poisson distribution  $P(S) = 4S \exp(-2S)$  [38]; histograms in a) and d) are almost perfect Wigner-Dyson ( $P(S) \sim S \exp(-S^2)$ ) and Poisson  $P(S) \sim \exp(-S)$  distributions. The distributions are  $j$ -dependent, that is an evidence of the interference of both kinds of fluctuations: finite-size ones and those of the excited level spacings

Therefore the impact of the second boson mode is that it essentially changes the quantum statistics. For the non-resonance case  $\Omega_1 \neq \Omega_2$  (Figure 3) we observe a considerable suppression of chaos manifesting in reduction of the “pure” domain of the Wigner-Dyson chaos in the space of the parameters  $\alpha, \beta$ . In the resonance case  $\Omega_1 = \Omega_2$  basically similar results as in our previous analysis [38] are recovered, the most important one being the complete disappearance of the domain of the Wigner-Dyson NNLS distribution. According to the results of Section 3 the reduction of the Wigner-Dyson chaos is to ascribe to quantum correlations (squeezing) in the radiation domain and the correlation (entanglement) of both the bosons.

Present results essentially deviate from the Wigner-Dyson statistics imposed by one-boson Dicke model [9]. For comparison, we performed the same calculations of NNLS distributions for the standard Dicke model (Figure 4). The distributions follow closely the Wigner-Dyson form of the  $P(S)$  curve independent of the choice of pairs of parameters  $\omega_0$  and  $\lambda$  in both the subcritical (normal) and supercritical (radiation) regions. Good agreement is achieved only for high values of  $j$ , finite-size fluctuations occur for small  $j$ .

To visualize the wave functions we considered their spreading over the electron levels and integrated out two boson degrees of freedom. Thus we found numerically

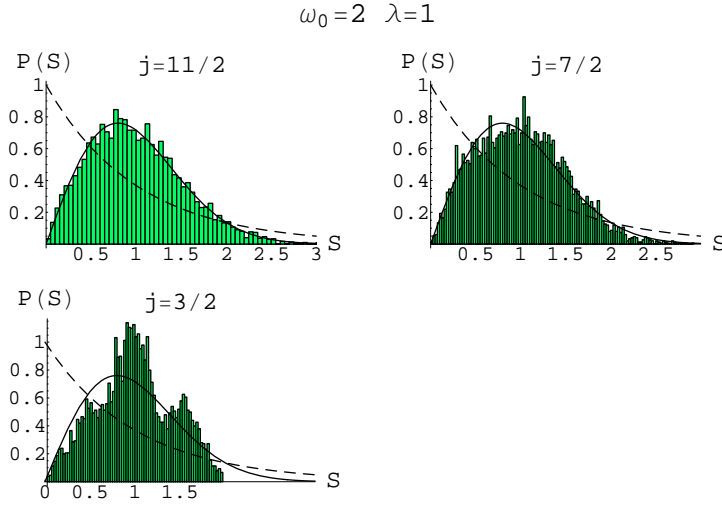


**Figure 4.** Level spacing distributions for one-boson Dicke model (4) (boson frequency  $\Omega$  scaled to 1). The parameters of the Dicke model (4) correspond to our parameters  $\alpha, \beta$  as  $\lambda \rightarrow \sqrt{\Omega_1/\Omega_2}\beta$ ,  $\omega_0 \rightarrow 4\alpha^2/\Omega_1$ . For sufficiently large  $j$ , the distribution is approaching the Wigner-Dyson distribution for any pairs of the parameters  $\lambda, \omega_0$  as one can see for  $j = 7/2, 11/2$ . The smaller  $j$ , the stronger are the nonuniversal fluctuations. Similarly to the previous Figure the  $j$ -dependence is the evidence for mixing of both kinds of fluctuations in the Dicke model.

the probability  $P_i^{(n)}$  of the wave function  $\phi_i^{(n)}$  to occupy a given electronic level  $i$  of the system. The full wavefunction depending on both vibron and electron level variables is calculated by the same scheme of the diagonalization of the quantum Hamiltonian in the representation of Fock states as described above. If  $\beta = 0$ , Hamiltonian equation is split onto  $N(= 2j + 1)$  independent equations labeled by  $i = 1, \dots, (2j + 1)$ , so that the wavefunction for each given state  $n$  is localized on some electron level  $i$ . If  $\beta \neq 0$ , Hamiltonian matrix is no more diagonal (since  $J_x$  is nondiagonal), so that its components get interacting. The resulting eigenfunction is in general  $(2j + 1)$ -fold function occupying each electronic level (see Section 2 for the discussion on normal and super-radiant phase in the thermodynamic limit). Let  $\chi_i^{(n)}(Q_1, Q_2)$  be the  $i$ -th component of the  $(2j + 1)$ -dimensional vector of the eigensolution of Hamiltonian matrix equation for  $n$ -th energy level in the "coordinate" representation ( $\hat{Q}_l \propto b_l^\dagger + b_l$ ,  $l = 1, 2$ ). Then the occupation probabilities of the  $i$ -th electronic level are  $P_i^{(n)} = \int \int |\chi_i^{(n)}|^2 dQ_1 dQ_2$ . In this representation we exemplify the wave functions in Figure 5 for the levels  $n = 1, 4$  and the parameters around the point of QPT  $\alpha = 2$ ,  $\beta = 1.95, 2.05$  and  $\Omega_1 = \Omega_2$ . The abrupt change in the shape of wavefunctions when going from normal to super-radiant phase is easily perceivable not only for the ground state, but for lowest excited states as well (in this example for  $n=4$ ). However, for higher excited states the wavefunctions generally spread over the whole available electron space, irrespective to the relation between  $\alpha$  and  $\beta$ . The last relation is also reflected in the statistical properties of levels: they are invariant with respect to the exchange  $\alpha \leftrightarrow \beta$ ,  $\Omega_1 \leftrightarrow \Omega_2$ , likewise it was already shown for the generalized JT model [38].

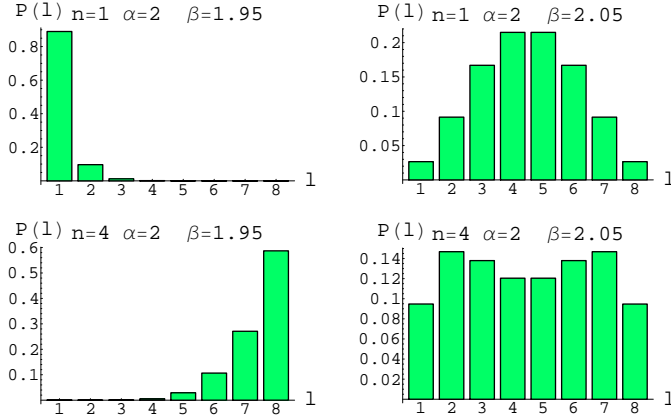


**Figure 5.** The occupations  $P(l)$  of the electronic levels  $l = 1, \dots, 2j + 1$  (see Sect. V) close the critical point  $\alpha = \beta$  ( $\Omega_1 = \Omega_2 = 1$ ;  $j = 7/2$ ) of the crossover between the quasi-normal and radiation domains for the ground  $n = 1$  and fourth  $n = 4$  excited state. For  $\Omega_1 \neq \Omega_2$  the occupations remain qualitatively the same.

In order to characterize quantitatively the behavior of the wavefunctions of excited states we introduce the entropy of level occupation

$$S_n = - \sum_{i=1}^N P_i^{(n)} \log P_i^{(n)}, \quad (30)$$

where  $\sum_{i=1}^N P_i^{(n)} = 1$ . In Figure 6 for  $\Omega_1 = \Omega_2$  we plot the said entropies for first 1000 quantum levels of a system with four electron levels ( $j = 3/2$ ). One can see from these figures that in the most excited states the electronic levels are equally populated (with probabilities  $1/(2j + 1)$ , e.g., last item in Figure (5)), thus the said entropies tend to their limiting value  $\log(2j + 1)$ . For four levels the entropy yields the value  $S_4 = 2 \log 2 = 1.38$  which is confirmed by Figure 6 for  $\alpha \neq \beta$ . However, among these extended states there emerge “localized” levels of lower values of the entropy which are characterized by relative localization of wavefunction on smaller number of electron levels. Such levels form marked branches seen in Figure 6, which remind the branches of “exotic” (localized) states similar to those found in our preceding paper [23]. Most of the states show an intermediate degree of localization between both the limits. These intermediate electronic states correspond to the critical mixed domain of the normal and radiation ones.

Another way to visualize the complex structure of the excited states and corresponding wave functions is the representation of the spectral density given by the imaginary part of the projected resolvent [24]. It shows the characteristic frequencies of the final state of the evolution of a system starting from the projected Hilbert space and returning to it. The spectral density of states  $F(E)$  can be defined with respect to some initially prepared state of the wave packet  $|\Psi_0\rangle$  and is related to the return probability to this state in the course of the system evolution through the exact states  $\Phi_n$ , eigenfunctions of the energies  $E_n$  of the system at small  $\varepsilon \simeq 0$ :

$$F(E) \equiv \text{Im} \langle \Psi_0 | (E - \hat{H} - i\varepsilon)^{-1} | \Psi_0 \rangle = \varepsilon \sum_n \frac{|\langle \Phi_n | \Psi_0 \rangle|^2}{(E - E_n)^2 + \varepsilon^2}, \quad (31)$$



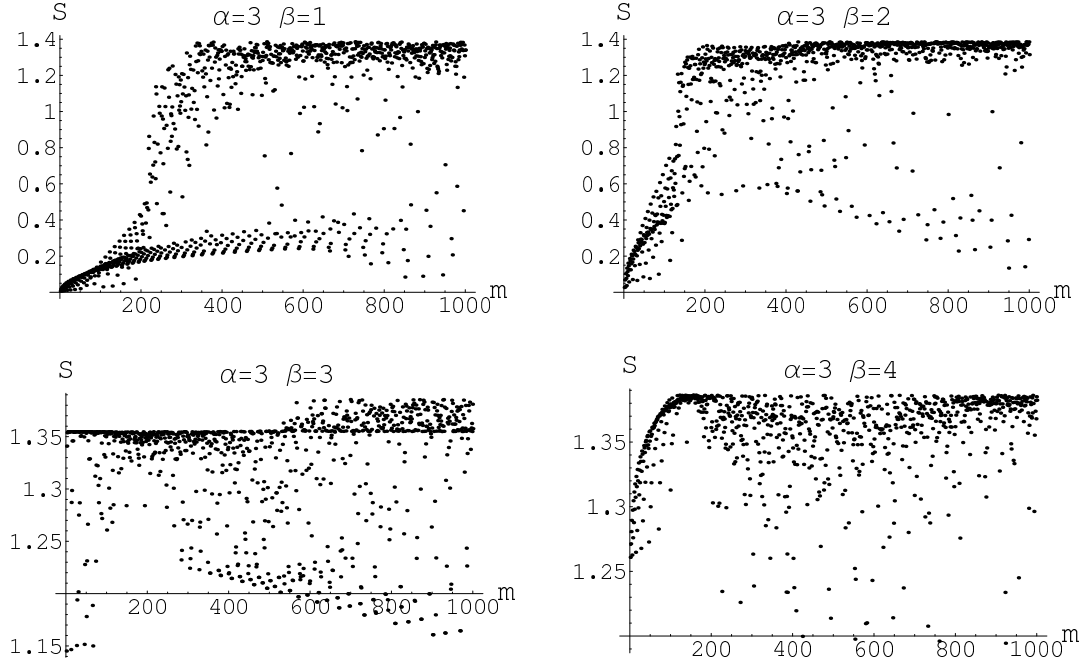


**Figure 6.** Entropies of occupation of electronic levels (30) as function of the number of the excited state  $m$  for  $j = 3/2$  (4 levels). The states with entropy lower than the limiting value  $\log(2j + 1)$  have larger measure of localization.

where  $|\Phi_n\rangle$  and  $E_n$  are the eigenfunctions and corresponding eigenvalues of Hamiltonian  $\hat{H}$ . The small parameter  $\varepsilon$  fixes the rules of handling the poles of the Green function in the complex space. In Figure 7 we show the examples of the spectral density for the values of parameters  $\alpha, \beta$  below and above the critical line. As the initial state  $|\Psi_0\rangle$  we took the ground state with  $\alpha = \beta = 0$ , that is the product of the electronic Dicke state  $|j, -j\rangle_{el}$  and the phonon state  $|0, 0\rangle_{ph}$  with zero number of both bosons 1 and 2. Thus the spectral density in Figure (7) characterizes the evolution of the system with the interactions  $\alpha, \beta$  switched on in the initial time. The peaks of each  $E_n$  measure overlap between the initial state  $\Psi_0$  and the eigenstate  $\Phi_n$  for  $\varepsilon \sim 0$ .

## 6. Conclusion

We performed analytical and numerical analyses of the multispin JT model with fully broken local rotation symmetry ( $\alpha \neq \beta$  and  $\Omega_1 \neq \Omega_2$ ).

Here, we will briefly summarize relations between the effects and their causes especially on the phase transition and statistical characteristics:

(i) Fluctuations in electron subsystem - finite-size fluctuations for small  $j$  occur mainly in the region close to the normal-radiation phase transition, Figs. 1, 2. Occupation of electronic levels close to the transition exhibits a partial excitation of the normal and dephasing of the radiation phase, Fig. 5. Thus, they smooth the phase transition point to a crossover region between the normal and radiation domains as a rather broad intermediate critical "mixed" domain. Similar finite-size effect for small  $j$

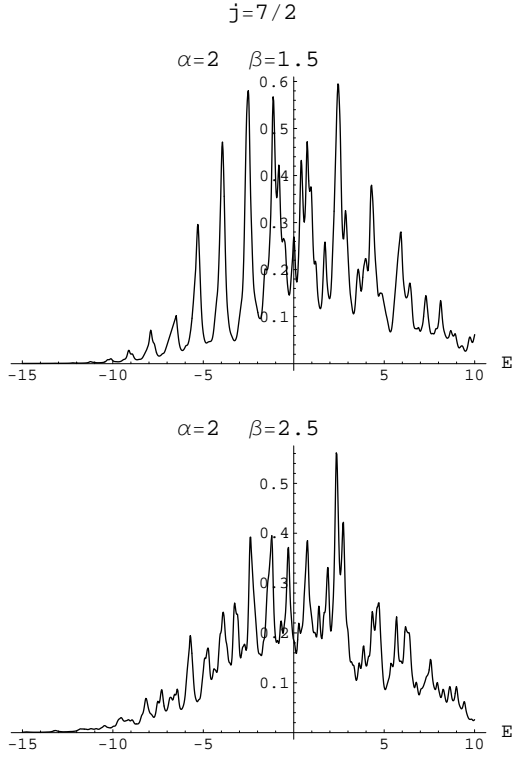


**Figure 7.** Examples of the spectral density of states  $F(E)$  (31) for  $\alpha = 2$  and  $\beta = 1.5, 2.5$  (We plot the resonant case  $\Omega_1 = \Omega_2 = 1$ ;  $j = 7/2$ ; the non-resonant cases do not change the picture qualitatively. The same applies for previous two figures.)

exhibits also the order parameter in the electron space  $\langle J_z \rangle / j$ , Fig.2.

The crossover of the wave functions: the excited states are spread over small number of sites in the "normal" domain to the macroscopic distribution of the excitation over the lattice in the radiation domain, Fig.5.

(ii) Fluctuations in the *excited boson subsystem*: The fluctuations of the nearest neighbour levels spacings are characterized by the distributions  $P(s)$ . Numerical results for  $P(s)$  (Fig.5) show markable perturbations for small values of the finite-size lattice parameter  $j$ . This is an evidence for the interplay of both kinds of fluctuations. In a semiclassical limit  $j \rightarrow \infty$  the perturbations of  $P(s)$  due to  $j$  vanish and the distributions are determined solely by the level repulsions (avoidings) moderated by the level correlations.

(iii) The difference in mode frequencies essentially contributes (besides the difference of the coupling constants) to the departure from the rotational symmetry of the underlying Hamiltonian. The additional (antisymmetric) boson mode mediates *correlations, mode squeezing and entanglement* by an assistance of the tunneling between the levels that weaken the level repulsions at small level spacings. They cause the nonuniversality of the distributions  $P(s)$  which is absent in the one-boson Dicke model.

The Holstein-Primakoff (HP) bosonization Ansatz in Section 3 makes it possible to describe the system as a system of three interacting bosons and find some useful, though approximate, analytical results. For a finite  $j$ , there opens a critical quantum "mixed" domain with partial occupation of the excitation space of all three coupled oscillators. This domain exists in the discrete Dicke model as well and vanishes in the semiclassical

limit  $j \rightarrow \infty$ .

The effective oscillators enable us to extract a sequence of repeated tunnelings in the radiation domain. The domain can be thus represented as an almost ideal instanton–anti-instanton phase (instanton lattice). *Each instanton represents a tunneling event, so that the radiation domain is the most chaotic one.* The dephasing mechanism in the radiation phase here is shown being caused by additional correlations from the neighbour instantons which perturb the ideal periodicity of the instanton lattice.

Several applications of the present two-boson finite-lattice system can be proposed:

(1) A zero temperature mechanism for interpretation of the coherence dephasing and the broadening of spectra [31, 32, 33, 34] and the broadening of the zero-phonon lines [35].

(2) A similar impact on the properties of ultracold atoms in optical lattices [24, 25, 39] due to the quantum localization-delocalization transition from the Mott insulator to the superfluid state. There the phase coherence of Bose atoms is destroyed by the suppression of the tunneling due to the localization by the strong lattice potential. From the competition of the tunneling and the localization due to the lattice there results the phase transition between the highly coherent superfluid phase of Bose atoms and the localized Mott insulating phase of the atoms on the lattice [39]. If quantum fluctuations can mediate the tunneling within the insulating phase, as well as perturb coherence of the superfluid phase, the system of Bose atoms in optical lattices would exhibit analogous properties as those of the two-boson Dicke model.

(3) Assistance of the additional coherent boson mode in the level splitting might be utilized as a possible mean to control chaos in related spectral properties of optical systems based on (pseudo)spin-boson models.

## Acknowledgments

The financial support by the project No. 2/0095/09 of the Grant Agency VEGA of the Slovak Academy of Sciences is highly acknowledged.

- [1] Graham P and Höhnerbach M 1984 *Z. Phys. B* **57** 233
- [2] Graham P and Höhnerbach M *Phys. Lett. A* **101** 61 (1984)
- [3] Lewenkopf C H, Nemes MC, Marvulle V, Pato M P and Wreszinski W F 1991 *Phys. Lett. A* **155** 113
- [4] Cibils M, Cuhe Y and Müller G 1995 *Z. Phys. B* **97** 565
- [5] Dicke R H 1954 *Phys. Rev.* **93** 99
- [6] Wang Y K and Hioe F T 1973 *Phys. Rev. A* **7** 831 ; Hepp K and Lieb E H 1973 *Phys. Rev. A* **8** 2517
- [7] Eastham P R and Littlewood P B 2000 *Solid State Comm.* **116** 357
- [8] Emary C and Brandes T 2003 *Phys. Rev. Lett.* **90** 044101
- [9] Emary C and Brandes T 2003 *Phys. Rev.* **E67** 066203
- [10] Harms K-D and Haake F 1990 *Z. Phys. B* **79** 159 ; Gnutzmann S, Haake F and Kus M 2000 *J. Phys. A* **33** 143
- [11] Tolkunov D and Solenov D 2007 *Phys. Rev. B* **75** 024402

- [12] Pfeifer P 1982 *Phys. Rev. A* **26** 701
- [13] Larson J 2008 *Phys. Rev. A* **78** 033833
- [14] Guhr T, Müller-Groeling A, Weidenmüller H A 1998 *Phys. Rep.* **299** 190
- [15] Kasprzak J, Richard M, Kundermann S, Baas A, Jeambrun P, Keeling J M J, Marchetti F M, Szyma M H, André R, Staehli J L, Savona V, Littlewood P B, Deveaud B and Dang Le Si 2006 *Nature* **443** 409
- [16] Eastham P R and Littlewood P B 2006 *Phys. Rev. B* **73** 085306
- [17] Keeling J 2007 *J. Phys.: Cond. Matter* **19** 295213
- [18] Love A P D, Krizhanowskii D N, Whittaker D M, Bouchekioua R, Sanvitto D, Al Rizeigi S, Bradley R, Skolnick M S, Eastham P R, André R and Dang Le Si 2008 *Phys. Rev. Lett.* **101** 067404
- [19] Dyson F J and Mehta M L 1963 *J. Math. Phys.* **4** 701
- [20] Majerníková E and Shpyrko S 2002, *Phys. Rev. B* **65** 174305
- [21] Majerníková E and Shpyrko S 2003 *J. Phys.: Cond. Matter* **15** 2137
- [22] Majerníková E and Shpyrko S 2008 *J. Phys. A: Math. Theor.* **41** 155102
- [23] Majerníková E and Shpyrko S 2006 *Phys. Rev. E* **73** 066215
- [24] Ziegler K 2005 *Phys. Rev. B* **72** 075120
- [25] R. Roth and K. Barnett 2004 *J. Phys. B: At. Mol. Opt. Phys.* **37** 3893
- [26] Vidal J and Dusuel S 2006 *Europhys. Lett.* **74** 817
- [27] Yuen H P 1976 *Phys. Rev. A* **13** 2226; Loudon R and Knight P L 1987 *J. Mod. Opt.* **34** 709-754
- [28] Gerlach B and Löwen H 1988 *Phys. Rev. B* **37** 8042 ; 1991 *Rev. Mod. Phys.* **63** 63
- [29] Eisert J, Plenio M B, Bose S and Hartley J 2004 *Phys. Rev. Lett.* **93** 190402
- [30] Longuet-Higgins H C, Öpik U, and Pryce M H L 1958 *Proc. Roy. Soc. London, Ser. A* **244** 1
- [31] Kuusmann I L, Liblik P K and Lushchik Ch B 1975 *JETP Lett.* **21** 72
- [32] Kmiecik H J, Schreiber M, Kloiber T, Kruse M and Zimmerer G 1987 *J. Lumin.* **38** 93
- [33] Kishigami-Tsujibayashi T, Toyoda K and T. Hayashi 1992 *Phys. Rev. B* **45** 13 737
- [34] Xiaoya Ding and Wright J C 1997 *Chem. Phys. Lett.* **269** 341
- [35] Malcuit M S, Maki J J, Simkin D J and Boyd R W, *Phys. Rev. Lett.* 1987 **59** 1189
- [36] Holstein T and Primakoff H 1949 *Phys. Rev.* **58** 1098
- [37] Brandes T 2005 *Phys. Repts* **408** 315
- [38] Majerníková E and Shpyrko S 2006 *Phys. Rev. E* **73** 057202
- [39] Fisher M P A, Weichman P B, Grinstein G and Fisher D S 1989 *Phys. Rev. B* **40** 546